



International Conference on Advances in Manufacturing and Materials Engineering,
AMME 2014

Surface characterization and machining of blind pockets on Ti6Al4V by abrasive water jet machining

Vijay Kumar Pal^{a*}, S.K. Choudhury^b

^aResearch scholar, Department of Mechanical Engineering, Indian Institute of Technology Kanpur, 208016, India

^bProfessor, Department of Mechanical Engineering, Indian Institute of Technology Kanpur, 208016, India

Abstract

Present work discusses the method of machining and characterization of blind pockets on Ti-6Al-4V alloy fabricated using Abrasive water jet machining (AWJM) by varying the process parameters; pressure, stand-off distance (SOD) and abrasive size. Depth of pockets was measured by coordinate measuring machine (CMM). Deeper pocket were formed at higher pressure; craters and high waviness were observed on machined surface. Surface waviness (SW) and craters sphericity were observed at many places of machined pocket through 3-D optical profilometer with objective lens (5x) and field of view (FOV 2x) along with the SPIP software. SW was found high at corners (side wall) of the pockets. Digital microscope of 230x and a scanning electron microscope (SEM) were used to observe and analyze the micro structure of the machined pockets.

© 2014 Elsevier Ltd. This is an open access article under the CC BY-NC-ND license

(<http://creativecommons.org/licenses/by-nc-nd/3.0/>).

Selection and peer-review under responsibility of Organizing Committee of AMME 2014

Keywords: AWJM; 3-D milling (blind pockets); surface waviness; crater sphericity; SEM

1. Introduction

Due to their unique properties, titanium alloys are widely used in industrial applications like aircraft turbine engine, aircraft structural components, aerospace fasteners, high performance automotive parts, marine application, bio medical devices etc. Abele et al., (2008) reported that machining of these alloys is difficult because they require much higher cutting forces in comparison to steels of equivalent hardness. Conventional machining of hard metals becomes more expensive in terms of tool wear and loss of quality in the product owing to induced residual stresses

* Corresponding author. Tel.: + 91-0512- 2597627; fax: + 91- 512- 2597408

E-mail address: vijayp@iitk.ac.in

during manufacture. Non-conventional methods were introduced to overcome most of the problems associated with the conventional machining. Processes like ultrasonic machining (USM), electro chemical machining (ECM), electric discharge machining (EDM), laser beam machining (LBM), electron beam machining (EBM) and water jet machining (WJM) etc. fall under this category. However most of the processes have several major limitations such as thermal damage to the machined material, poor edge quality, material property constraints, slow machining time etc. Masuzawa et al., (1985-86). Abrasive water jet machining (AWJM) is one of the most promising non-conventional machining processes, which has capacity to machine any material ranging from soft to hard without considering any special material property (Electrical conductivity) or having any tool design problem. It is a non-conventional machining process in which a mixture of abrasive particles with high pressure water is converted to a high velocity jet for cutting. The high speed abrasive water jet machining employs the erosion phenomenon for material removal when the abrasive particles along with high velocity water hit the target surface explained by Finnie, (1960). Less fixture requirements and heat affected zones due to no contact between the cutting tool and work piece are some of the major advantages of this technique. Process primarily depends on the following input parameters – abrasive flow rate, traverse speed, standoff distance (SOD), water jet pressure, shape and size of abrasive particles. This process is well established for through cutting and most of the works reported was based on through cutting by AWJM.

Now-a-days, researchers have also started experimenting on generating blind features using AWJM. For generating blind features like pockets and channels, several authors used the multiple passes linear traverse cutting as milling strategy. This principle is based on the superposition of several passes to obtain a cavity of defined geometry. The lateral distance between the single kerf/passes is the main parameter in this process (Laurinat et al., 1993), which is kept less than the diameter of the jet (d). Hashish (1994) used the principles of rotary table and masking to perform a controlled depth milling of iso-grid structures. Fowler et al., (2003) have developed the process of controlled depth milling CDM and studied the effects of various parameters like traverse speed, jet impingement angle, milling direction, grit size, etc. on surface characteristics while machining titanium alloy. Pal and Tandon., (2011) studied the role of machinability in AWJ-CDM for materials like AL 6061 alloy, AL 2024, Brass 353, Titanium AISI 304 (SS) and Tool Steel. The authors observed that, time taken to mill increases as the depth of milling increases non-linearly due to loss of energy of jet and increase in standoff distance (SOD). In water jet milling the pump pressure was found to be a more prominent parameter and quality of surface generated defined by depth of cut, tolerance and roughness of bottom (Momber et al., 1996).

The objective of the present work is to generate pockets on titanium alloy (Ti-6Al-4V) with operating parameters, such as pressure, standoff distance and abrasive size. Here the depth of the pockets was measured by coordinate measuring machine (CMM). Machined surface was scanned through 3-D optical profilometer with objective lens (5x) and field of view (FOV 2x) along with the scanning probe image processing (SPIP) software. Surface waviness, roughness and crater were measured at different locations of the pockets. Crater sphericity was found closer to one because of 900 impact of the jet. Surfaces waviness was observed more at the corners of the pockets (side wall) as compare to other portions of the pockets. More depth and volumetric MRR was found at higher pressure, because of high kinetic energy of jet. Finally microscopic study of machined surface has been performed with the help of digital microscope (230x) and scanning electron microscope (SEM).

2. Experimental details

2.1. Methodology to fabricate blind pockets

The pockets were generated by using the superposition of kerfs as milling strategy; the path followed in present work was rectangular raster as shown in Fig. 1. Overlapping was done by keeping the distance between the two consecutive passes, i.e., step-over (SO) less than the diameter (d) of the nozzle. Fig. 1 shows the paths that were adopted and executed during AWJ-CDM. Here, the dot indicates the starting point of motion. At every pass of nozzle jet, the diameter of impingement (i.e. exposure of jet) overlaps and removes the material to generate pocket.

2.2. Experimental setup

The experiments were conducted on a Ti-6Al-4V alloy of 5 mm thickness sheet with commercial abrasive water jet machine (OMAX Corp.) available in the laboratory (Fig. 2). This work aims to achieve a blind pocket of size 25 mm x 25 mm x 1 mm. To hold the specimen on the machine and keeping SOD, suitable fixture and gauges were designed. In the software provided with the machine, the values of input parameters like abrasive flow rate, pressure etc. were provided and the etch speed (traverse speed) was suggested. Two process parameters, namely pressure and standoff distance were varied at three levels and another parameter of abrasive size was varied at two levels (due to unavailability of supply). The range of process parameters and their level are given in Table 1. Based on the process parameters considered and using a full factorial design, a total number of 18 experiments were conducted. In the given setup, the optimum values of parameter like abrasive flow rate was considered based on standard operating conditions of AWJ machine available.

Table 1. Operating parameters with their ranges

Pressure (kpsi)	Abrasive size (Mesh)	SOD (mm)
15-25-35	80# & 120#	2-3-4
15-25-35	80# & 120#	2-3-4
15-25-35	80# & 120#	2-3-4

Extensive preliminary experiments were carried out to determine the operating ranges of the input parameters. All the experiments were conducted at a 90° impingement angle and the traverse speed of nozzle movement was kept at 2966 mm/min (suggested by software). The orifice and the mixing tube were kept same throughout the experimentation. Table 2 shows the specifications of the machine. The basic objective of the work was to explore the effect of process parameters in controlling the responses like MRR and depth of pocket and the surface quality of the pocket.

Table 2 Machine specification

Jet impingement angle	90°
Orifice diameter	0.33 mm
Abrasive flow rate	0.226 kg/min
Mixing tube diameter	0.762 mm
Mixing tube length	101.6 mm
Maximum working pressure	310 MPa

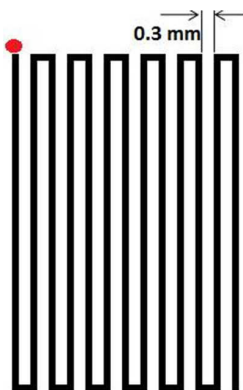


Fig. 1 Path followed in CDM

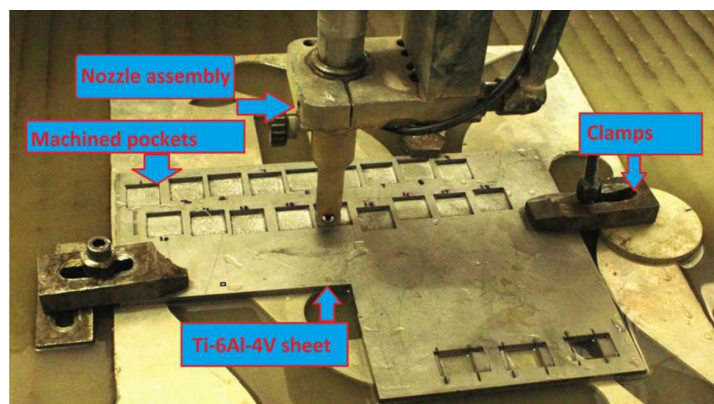


Fig. 2 Experimental setup

3. Measuring instruments

3.1. Coordinate measuring machine (CMM).

CMM was used to measure the dimensions of the pockets. Depth of pockets was measured through manual control of the probe. The probe attached with the third axis of machine, which is sensory part of a CMM responsible for measuring depth of pockets in present study (Fig. 3). The difference between two planes (base of pocket and top surface of plate) was calculated. Data was obtained through CMM with the help of software available with the machine. It was considered that base and side wall of pockets were uniform flat surface (Neglecting undercuts in present analysis as an assumption). Using this assumption, the volume of material removed in pockets was estimated.

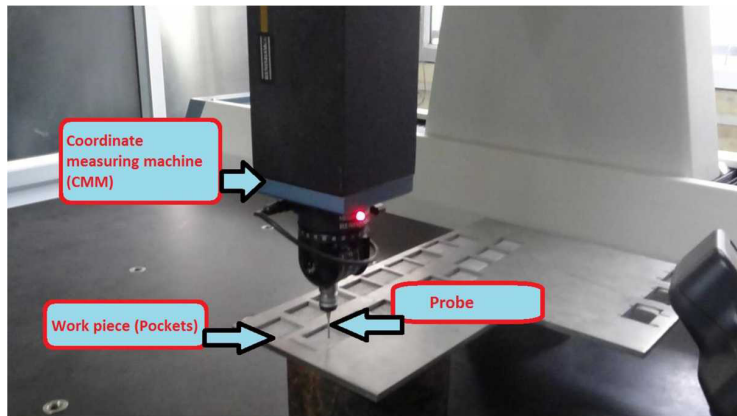


Fig. 3 Measurement of pocket depth through Coordinate measuring machine (CMM)

3.2. 3-D optical profilometer

Machined surface (base) of pockets was scanned through a 3-D optical profilometer embedded with the scanning probe image processing (SPIP) software. Optical profilometer, having a large scanning range, generates high resolution 3D and 2D images. Objective lens (5X) and FOV (2X) were used in the optical profilometer. Scanned process of the machined surface is shown in Fig. 4.

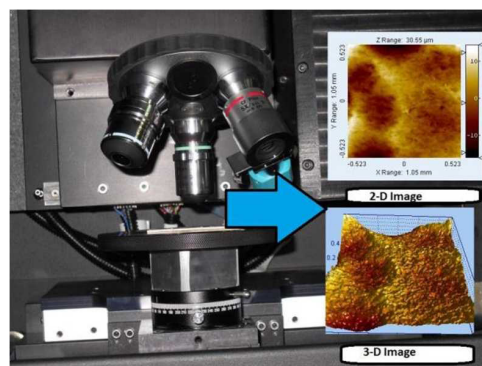


Fig. 4 Optical profilometer 3-(d) images of pockets

Surface waviness was observed on different places of the pockets (machined surface). Digital microscope of 230x was used to observe the nature of the machined surface and details were studied by scanning electron microscope (SEM), Model-FESEM SUPRA 40 VP CAL ZEISS.

4. Observation and Results

Experimental results and measurement data are presented in this section. Based on the measurement, depth of pockets and their volume were calculated and tabulated (Table 3). The average value of surface roughness was found in the range of 6-10 microns on all the machined surfaces.

Table.3 Observation Table

Pressure (KPsi)	SOD (mm)	Abrasive mesh(#)	Depth (mm)	MRR(mm ³ /sec)
15	2	80	1.10	6.88
15	3	80	1.15	7.19
15	4	80	1.21	7.56
25	2	80	1.85	11.56
25	3	80	1.80	11.25
25	4	80	1.81	11.31
35	2	80	1.92	12.00
35	3	80	2.21	13.81
35	4	80	2.91	18.19
15	2	120	1.08	6.75
15	3	120	1.10	6.88
15	4	120	1.05	6.56
25	2	120	1.60	10.00
25	3	120	1.61	10.06
25	4	120	1.80	11.25
35	2	120	1.95	12.19
35	3	120	2.0	12.50
35	4	120	1.62	10.13

4.1. Effect of parameters on pockets depth and MRR

In this section, effect of process parameters on depth of pocket and MRR is discussed based on the responses observed by experimentation and characterization of the samples. Volumetric MRR were plotted against pressure and standoff distance with two abrasive sizes (80# and 120#). It is very observed that as the pressure increases, the depth of the pocket increases due to high kinetic energy of the jet. Depth of the pocket is also slightly affected by the standoff distance (SOD), but no prominent effect was observed in present range of SOD (2 to 4 mm). It was also found that, as the size of the abrasive particles increases, the depth achieved was more because of the higher energy of impact. Depth of pocket and volumetric MRR follow same trend because area of pocket was kept constant (25x25 mm)

Fig. 5 (a) and Fig. 5(b) show the effect of pressure on volumetric MRR for two grit sizes.it can be seen that MRR for both abrasive grit sizes is high at larger pressure and decreases with decrease in pressure. The maximum MRR is (18.187 mm³/sec) with grit size of 80# and approximately (12.50 mm³/sec) with grit size 120#.

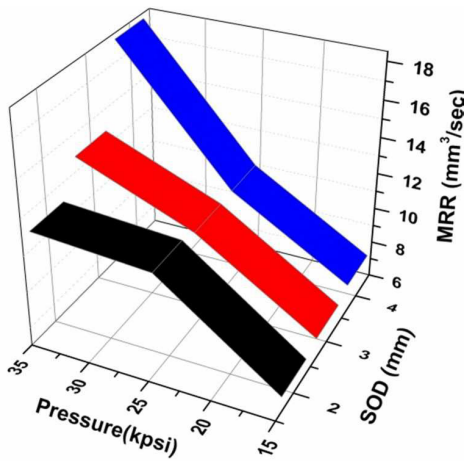


Fig. 5(a) Effect of parameters on volumetric MRR for abrasive (80#)

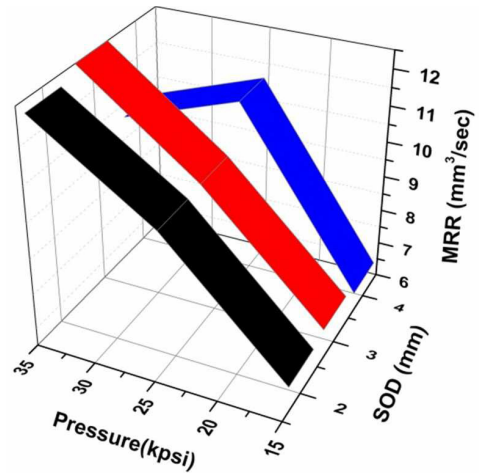


Fig. 5(b) Effect of parameters on volumetric MRR for abrasive (120#)

4.2 Surface characterization and material removal in pocket machining by AWJM

Present work deals with machining of blind pockets, where jet restricts to flow out from the work piece surface. It was found that, pocket surfaces were not very uniform. This can be explained by the fact that, erosion might have caused by number of non-identical abrasive particle which causes unbalanced erosion. In present work, machined surface was scanned through 3-d optical profilometer as discussed in section 3. It can be seen in the Figure 6(c), that crater of hemispherical shape was found on machined surface. The waviness on machined surface was observed. It was found that at the corner of the pocket (side wall), the effect was more prominent, i.e., high waviness was observed as compared to other surface of the pockets (Fig. 6(a), (b)). This might have caused of stress concentration at the corners were more as compare to rest portion of pocket, which causes the change of deformation at the corners.

In order to understand the crater sphericity, sufficient attempted have been made using numerical methods. M. Takaffoli, (2009) and Shukla M, (2012) studied the 20 particle impact FEM simulation. He also observed that at 90 degree, the sphericity evaluated at top surface remains closer to one, irrespective of particle velocity. Similar observation (Fig. 6(c)) was found experimentally in the present work.

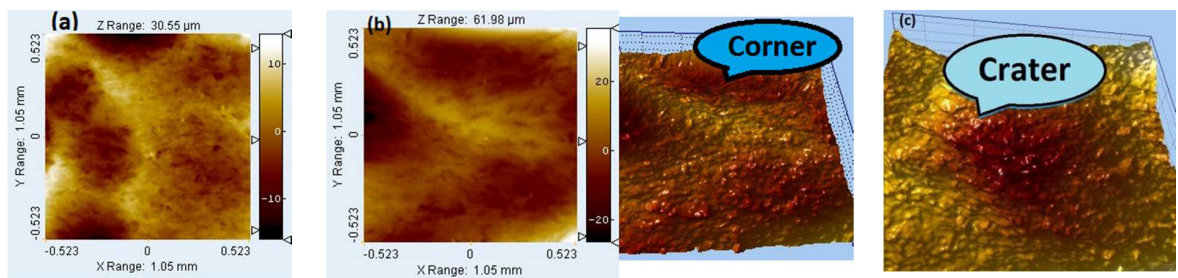


Fig. 6. Scanned Surface, (3-d) images of pockets at (a) mid surface (b) Corner and (c) Crater formed at machined surface

SEM images study focuses on micro-investigation of the machined surface (erosion) at different operating conditions. Higher magnifications SEM micro-graphs were taken for depth analysis of erosion phenomena. It can be seen from the Fig. 7 and Fig. 8 that the erosion magnitude increases as well as surface morphology changes with increase in pressure because change or increase in pressure causes the change in surface morphology in terms of level of grit embedment. From Fig. 9, it was observed that at lower abrasive size, surface finish was quite good as

compared to larger grit. This can be explained by the fact that smaller particle generating smaller irregularities on the machined surfaces.

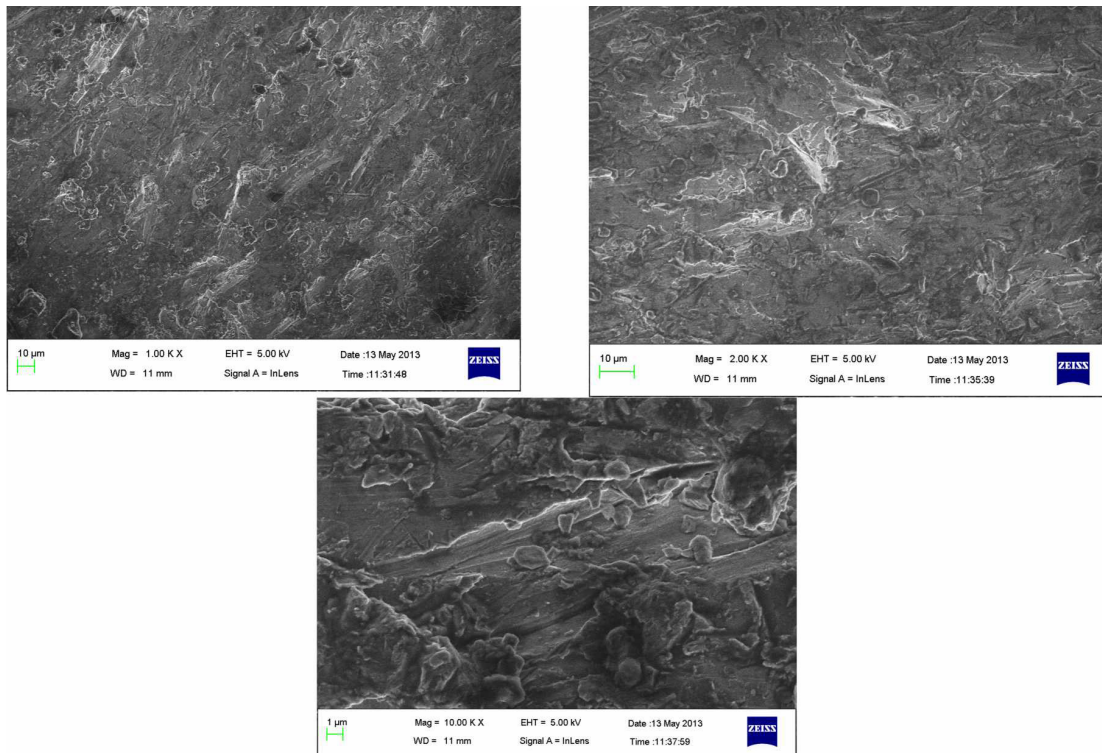


Fig. 7. SEM images of pockets surface at low pressure (15 Kpsi), small SOD (2 mm) of 80# garnet

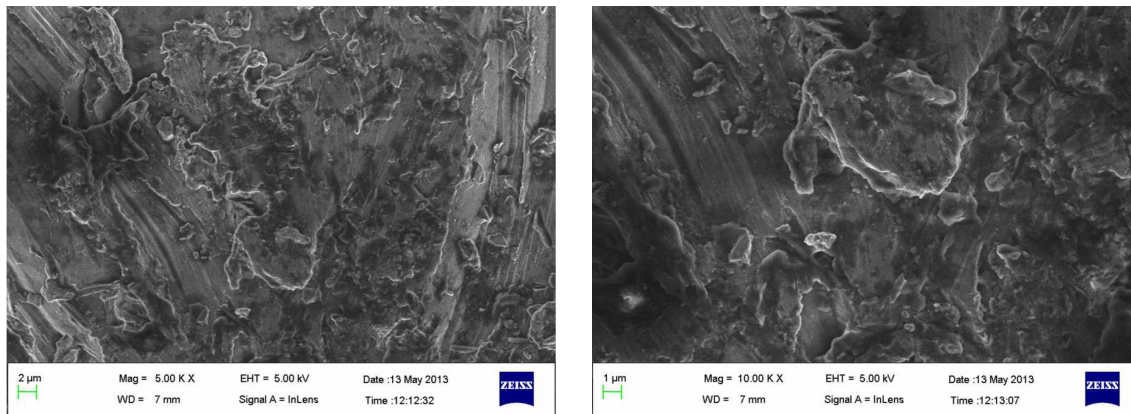


Fig. 8. SEM images of pockets surface at high pressure (35 Kpsi), large SOD (4 mm) of 80# garnet

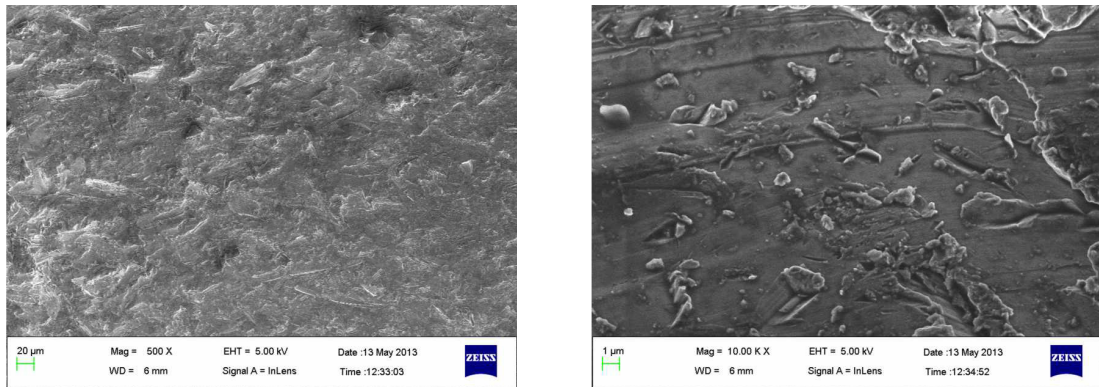


Fig. 9. SEM images of pockets surface at low pressure (15 Kpsi), large SOD (4 mm) of 120# garnet

5. Conclusions

In this paper, surface morphology of blind pocket machining by AWJM process was also studied. In blind pocket machining, pockets were fabricated by controlling parameters of the process. From the 3D scanned surfaces, high waviness and roughness was observed on machine surface. Based on the experiments and microscopic investigation following conclusions are drawn:

- High waviness was found at corners of the pockets (side wall), because first pass of raster path overlaps only with one side of another path (consecutive path), which creates more waviness on the surface.
- The depth and MRR was more at higher pressure because of high kinetic energy of jet.
- Rough surfaces were found on pockets because of non-identical abrasive particles plays role on material removal. Low waviness was found at rest of the surfaces of pockets than corner surfaces because at corners stress concentration was more as compare to rest area of machined pockets.
- SEM images shows that, surface morphology of the machined surface changes at different pressure.
- Crater sphericity was found to closer to 1, because of 90° impact of jet.
- Small abrasive size gives quite good surface as compared to larger grit because, smaller particle generating smaller irregularities on the machined surfaces.

References

- Abele, E., Frohlich, B., 2008. High speed milling of titanium alloys. *Advancement in production energy and management* (3):131-140.
- Finnie, I., 1960. Erosion of surfaces by solid particles. *Wear* (3): 87-103.
- Fowler, G., Shipway, P.H., Pashby, I.R., 2005. A technical note on grit embedment following abrasive water jet milling of titanium alloy. *Journal of Material Processing Technology* (159): 356-368.
- Hashish, M., 1994. *Controlled-depth Milling Techniques Using Abrasive-Waterjets*. In: Allen N G (ed) 1994 *Jet Cutting Technology*, Mechanical Engineering Publication Ltd, London. 449-461.
- Hutchings, I.M., 1974. Article erosion of ductile metals: a mechanism of material removal, *Wear* 27: 121.
- Kagaya, K., Oishi, Y., K., Yada., 1986. Micro-electro discharge machining using water as working fluid, micro-hole drilling. *Precision engineering* 8(3): 156-162.
- K. Naresh, S. Mukul, 2012. Finite element analysis of multi-particle impact on erosion in abrasive water jet machining of titanium alloy, *Journal of computational and applied mathematics* 236 : 4600-4610.
- Laurinat, A., Louis, H., Meier-Wiechert, G., 1993. A Model for Milling with Abrasive Water Jet In: Hashish M (ed.) 1993 *Proceedings of the 7th American Water Jet (1)*, Water jet Association, St. Luis, 119-139.
- Momber, A.W., Eusch, I., Kovacevic, R., 1996. Machining refractory ceramics with abrasive water jet. *Journal of Material Science*. 31: 6485-6493.
- Masuzawa, T., Fujino, M., Kobayashi, K., Suzuki, T., 1985. Wire Electric discharge grinding for micro-machining. *Annals of the CIRP* 34(1): 431-434.

- Masuzawa, T., Yamamoto, M., Fujino, M., 1986. A micro punching system using wire-EDM, Proceedings of the international symposium for electromachining (ISEM-9): 86-89.
- M. Takaffoli, M. Papini, 2009. Finite element analysis of single impacts of angular particles on ductile targets, *Wear* 267. 144–151.
- Pal, V K., Tandon, P., 2011. Identification of role of machinability and milling depth on machining time in controlled depth milling using abrasive water jet. *International Journal of Advanced Manufacturing Technology*, 66:877-881.